

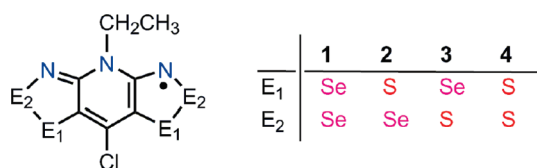
Magnetic Anisotropy in a Heavy Atom Radical Ferromagnet

Stephen M. Winter,[†] Saiti Datta,[‡] Stephen Hill,[‡] and Richard T. Oakley^{*,†}[†]Department of Chemistry, University of Waterloo, Waterloo, Ontario, Canada N2L 3G1[‡]National High Magnetic Field Laboratory and Department of Physics, Florida State University, Tallahassee, Florida 32310, United States

ABSTRACT: High-field, single-crystal EPR spectroscopy on a tetragonal bisdiselenazoyl ferromagnet has provided evidence for the presence of easy-axis magnetic anisotropy, with the crystallographic *c* axis as the easy axis and the *ab* plane as the hard plane. The observation of a zero-field gap in the resonance frequency is interpreted in terms of an anisotropy field several orders of magnitude larger than that observed in light-heteroatom, nonmetallic ferromagnets and comparable (on a per-site basis) to that observed in hexagonal close packed cobalt. The results indicate that large spin–orbit-induced magnetic anisotropies, typically associated with 3d-orbital-based ferromagnets, can also be found in heavy p-block radicals, suggesting that there may be major opportunities for the development of heavy p-block organic magnetic materials.

The magnetic properties of light heteroatom organic radicals such as nitroxyls, verdazyls, and thiazyls have been the subject of extensive research for over 30 years.¹ This work has revealed a few systems that undergo ferromagnetic ordering, but their Curie temperatures (T_C) are all below 2 K.² Nonmetal-based radical ion salts displaying higher ordering temperatures have also been reported,³ with that of the TDAE·C₆₀ complex ($T_C = 16$ K) being the highest.⁴ However, for none of these materials (neutral or charged) is the observed coercive field (H_c) more than a few oersteds.⁵ In light of these results, the discovery of bulk ferromagnetism in heterocyclic bisdiselenazoyl radical **1** (Chart 1),⁶ for which $T_C = 17$ K and $H_c = 1370$ Oe at 2 K, represents a significant advance in the development of nonmetal-based magnetic materials.

Chart 1



Radical **1** and its isostructural sulfur/selenium-containing variants **2–4** crystallize in the noncentric tetragonal space group $P4_21m$ (Figure 1).^{6,7} The structure consists of pinwheel-like clusters of radicals arranged about $\bar{4}$ centers, with each of the four radicals within the pinwheel providing the basis for a slipped π -stacked array running parallel to the *c* axis. Previous studies have established that the presence of the heavier chalcogen is crucial for achieving a high magnetic ordering temperature. For

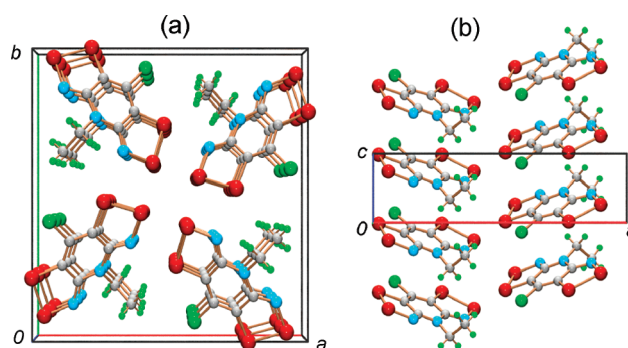


Figure 1. Crystal packing of **1** viewed (a) parallel and (b) perpendicular to the π -stacking direction. Radicals **2**, **3**, and **4** are isostructural to **1**.

example, T_C for the all-selenium radical **1** is greater than that for the mixed S/Se variant **2** (13 K). The other mixed S/Se system **3** also undergoes ordering, although it is a spin-canted antiferromagnet with a Néel temperature (T_N) of 14 K. There is no evidence for magnetic ordering down to 2 K in the purely sulfur-based material **4**. The increase in ordering temperature with selenium incorporation can be understood in terms of enhancement of the isotropic through-space magnetic exchange interactions occasioned by the presence of more diffuse magnetic orbitals (i.e., 4p for selenium vs 3p for sulfur).⁸ What remains to be explained is the source of the magnetic anisotropy that gives rise to the large coercive field in **1**. In contrast to $S > 1/2$ metal-based systems, where anisotropy is often a property of individual ions, Kramer's theorem forbids zero-field anisotropy for single $S = 1/2$ radicals. Thus, in the case of **1**, the anisotropy must arise from interactions between the radicals.

To explore this issue we used ferromagnetic resonance (FMR) absorption to provide an independent measure of the solid-state magnetic anisotropy in **1**.⁹ The theory of resonance absorption of microwaves by magnetically ordered phases is well established,¹² and the technique has been applied to the study of many materials,¹³ including radicals.¹⁴ The basis of its utility is that the resonance conditions are highly sensitive to the angular variation of the free energy associated with magnetic spins.

In tetragonal crystals, the lowest-order anisotropic contribution is uniaxial, and the free energy density F associated with the bulk ferromagnetic magnetization \mathbf{M} may be written as

$$F = -\mathbf{M} \cdot \mathbf{H}_{\text{ext}} - K \cos^2 \theta_M - O(\cos^4 \theta_M) - O(\cos 4\phi_M \sin^4 \theta_M) \quad (1)$$

Received: March 9, 2011

Published: May 09, 2011

where \mathbf{H}_{ext} is the external field, K is the second-order anisotropy constant, and θ_M and ϕ_M are the polar and azimuthal angles defining the direction of \mathbf{M} with respect to the crystallographic c axis.⁹ For an anisotropy field $H_A = 2K/M > 0$, there is a preference for magnetization along the crystallographic c axis (easy-axis anisotropy), whereas $H_A < 0$ denotes a preference for orientation in the ab plane (easy-plane anisotropy). Experimentally, the coercive field H_c is typically found to be between 10% and 40% of H_A .¹⁵ When only the second-order term is included, in the high-field limit ($|\mathbf{H}_{\text{ext}}| \gg H_A$) for a fixed microwave frequency f , the external resonance field should vary as

$$|\mathbf{H}_{\text{ext}}| \approx \frac{f}{\gamma} - \frac{1}{2} H_A (3 \cos^2 \theta - 1) \quad (2)$$

where θ gives the orientation of the external field with respect to the crystallographic c axis. The higher-order free energy terms, which are associated with the anisotropy in the ab plane, introduce higher $\cos^4 \theta$ and $\sin^4 \theta$ terms in this high-field limit. Measurements of the resonance field as a function of the crystal orientation performed at high field (Figure 2a) were consistent with eq 2, indicating negligible higher-order components and therefore negligible anisotropy in the ab plane. Given $H_A > 0$, we have identified **1** as a uniaxial easy-axis ferromagnet whose easy axis lies along the crystallographic c axis.

To confirm this result, the FMR response was compared to exact expressions for the resonance condition that can easily be deduced for the parallel (eq 3) and perpendicular (eq 4) orientations of the external field. For \mathbf{H}_{ext} parallel to the c axis ($\theta = 0$),

$$f = \gamma(H_{\text{ext}} + H_A) \quad (3)$$

while for \mathbf{H}_{ext} perpendicular to the c axis ($\theta = \pi/2$),

$$f = \begin{cases} \gamma(H_A^2 - H_{\text{ext}}^2)^{1/2} & H_{\text{ext}} \leq H_A \\ \gamma[H_{\text{ext}}(H_{\text{ext}} - H_A)]^{1/2} & H_{\text{ext}} \geq H_A \end{cases} \quad (4)$$

The observed multi-high-frequency response for **1** (shown in Figure 2b for $T = 10$ K) conformed to the anticipated results. The variations in the magnitude of H_A , as extracted from fits of eqs 3 and 4 to data collected at three different frequencies (50.4, 66.9, and 240 GHz) and several temperatures, indicated that the anisotropy field grew with decreasing temperature to a maximum of 8.2 kOe at 5 K (Figure 2c). The observed anisotropy field was several orders of magnitude larger than that observed for light atom organic ferromagnets such as TDAE·C₆₀ ($H_A = 0.058$ kOe at 5 K¹⁶) and β -p-NPNN ($H_A = 0.12$ kOe at 0.4 K¹⁷). Indeed, if magnetic saturation is assumed, the data for **1** provide an anisotropy constant (K) of 2.4×10^{-5} eV/molecule at 5 K, which is comparable to the value of 5×10^{-5} eV/atom measured for bulk hexagonal close packed cobalt at 4.2 K.¹⁸ From this we conclude that the magnitude of the anisotropy observed here for a 4p-based radical ferromagnet is similar on a per-site basis to the anisotropy observed for noncubic 3d transition metal ferromagnets.

In homogeneous magnetic materials, the anisotropy field H_A may be viewed in terms of contributions arising from (i) molecular spin dipole–dipole interactions (H_A^{dip}), (ii) macroscopic demagnetizing fields (H_A^{dem}) (for nonspherical crystals), and (iii) spin–orbit effects (H_A^{SO}) (eq 5):

$$H_A = H_A^{\text{dip}} + H_A^{\text{dem}} + H_A^{\text{SO}} \quad (5)$$

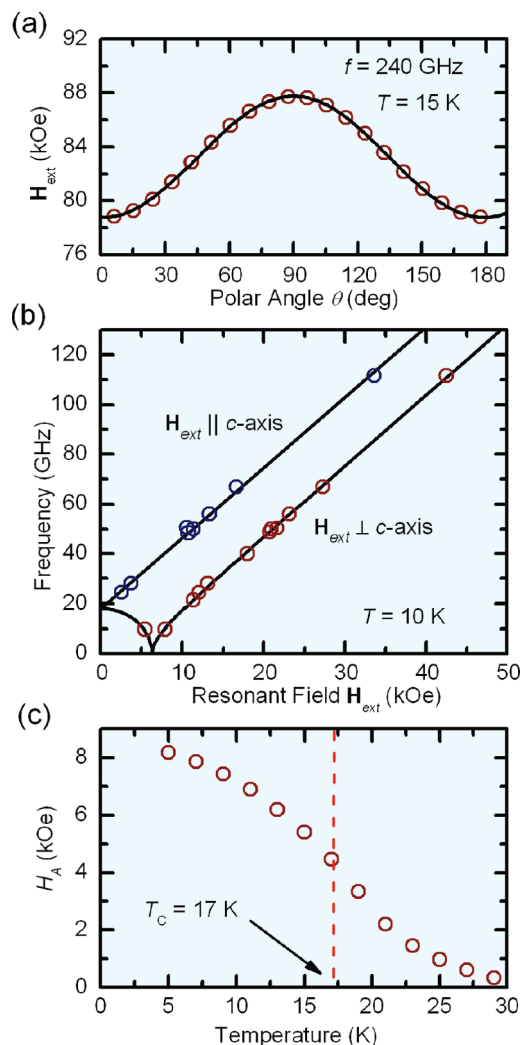


Figure 2. (a) Observed high-field angular dependence of the resonance field for **1** at $T = 15$ K (open circles). The data is fitted with a $\cos^2 \theta$ curve, in accord with eq 2 (solid line). (b) Observed resonance field versus frequency for **1** at $T = 10$ K (open circles). The solid lines represent fits of eqs 3 and 4. (c) Anisotropy field of **1** as a function of temperature. The curve displays an apparent inflection point near the ferromagnetic transition temperature $T_C = 17$ K.

Of these, the first term depends on the microscopic distribution of spins in the lattice and, in the case of **1**, should favor alignment of \mathbf{M} along the c axis (i.e., the axis of highest linear spin density). Although the magnitude of this effect can be estimated numerically by using Ewald summation techniques,¹⁹ it should by inspection be on the same order of magnitude as the total anisotropy field H_A measured for spherical samples of β -p-NPNN, for which the demagnetizing and spin–orbit effects are negligible. On this basis, it is reasonable to conclude that H_A^{dip} in **1** is ~ 0.1 kOe. The second dipolar effect, the shape-dependent demagnetizing field H_A^{dem} , which is often substantial in transition-metal materials, is also small as a result of the low density of spins in **1** (and any organic magnet). Indeed, approximating the needlelike crystals of **1** as cylinders of infinite length suggests that $H_A^{\text{dem}} = \mu_0 M/2$, which affords a contribution of only 0.1 kOe assuming magnetic saturation. It is therefore our interpretation that the dipole contribution $H_A^{\text{dip}} + H_A^{\text{dem}}$ is not sufficient to explain

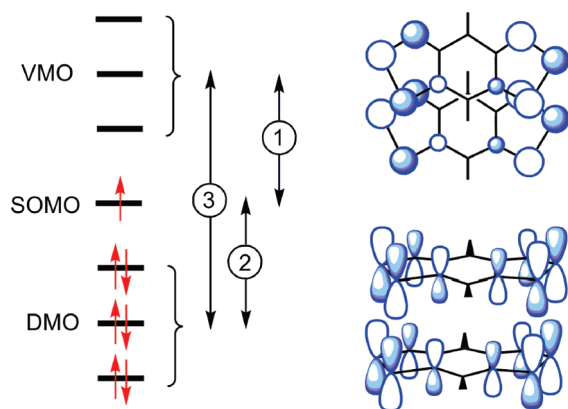


Figure 3. (left) The three types of electronic transitions induced by H_A^{SO} . (right) Near-orthogonal overlap of radical SOMOs along the π stacks: (top) top view; (bottom) side view.

the magnetic anisotropy in **1**, contrary to what is found for light-element organic magnets.²⁰ This leaves spin–orbit effects H_A^{SO} as the only plausible cause for the large anisotropy observed.

Magnetic anisotropy arises from spin–orbit effects due to coupling between the spin (S) and orbital (L) angular momentum degrees of freedom, which may be represented phenomenologically by the Hamiltonian $\hat{H}_{\text{SO}} = \lambda \hat{L} \cdot \hat{S}$, the strength of which grows sharply with atomic number (roughly as Z^4).²¹ At a single site, this coupling mixes states through virtual electronic transitions between the singly occupied, doubly occupied, and virtual molecular orbitals (SOMOs, DMOs, and VMOs), as illustrated in Figure 3. The resulting mixed states are eigenstates of the total angular momentum $\mathbf{J} = \mathbf{L} + \mathbf{S}$ and are characterized by anisotropic molecular \mathbf{g} tensors, as observed for diselenazoyl radicals.²² To first-order in spin–orbit coupling, the electronic state of the magnetic electron on each radical is a perturbation of the SOMO, $|\psi_0\rangle$,²³ as shown in eq 6:

$$|\psi_0^{(1)}\rangle = |\psi_0^{(0)}\rangle + \lambda \sum_n \frac{\langle \psi_n^{(0)} | \hat{L} \cdot \hat{S} | \psi_0^{(0)} \rangle}{\epsilon_n - \epsilon_0} |\psi_n^{(0)}\rangle \quad (6)$$

In the solid state, magnetic interactions that result from virtual hopping of electrons between these mixed states are also anisotropic. Moriya²⁴ used a perturbative approach to show that the resulting spin Hamiltonian \hat{H}_{ij} takes the form shown in eq 7,

$$\hat{H}_{ij} = -J_{ij} \hat{S}_i \cdot \hat{S}_j + \mathbf{D}_{ij} \cdot (\hat{S}_i \times \hat{S}_j) + \hat{S}_i \cdot \mathbf{\Gamma}_{ij} \cdot \hat{S}_j \quad (7)$$

where the order of the terms can be approximated by eq 8:

$$\hat{H}_{ij} \sim \left(2Q - \frac{4t_{00}^2}{U} \right) + O\left(\frac{t_{00} |C_{00}|}{U} \right) + O\left(\frac{|C_{00}|^2}{U} \right) \quad (8)$$

The first term in eq 7 represents the Heisenberg exchange interaction, which is represented in eq 8 by ferromagnetic (Q) and antiferromagnetic ($4t_{00}^2/U$) components, where Q is the direct exchange integral, t_{00} is the transfer (resonance) integral between SOMOs on adjacent radicals, and U is the Hubbard onsite Coulomb repulsion.²⁵ The second term, which is first-order with respect to the spin–orbit correction λ , involves the vector \mathbf{D}_{ij} representing the celebrated antisymmetric Dzyaloshinsky–Moriya (DM) interaction, which has been suggested to be responsible for the noncollinear spin arrangements

of centrosymmetric heavy atom organic antiferromagnets.²⁶ The third term, which is second-order in λ , involves the $\mathbf{\Gamma}_{ij}$ tensor and gives rise to the pseudo-dipolar anisotropic exchange (AE) interaction. Both DM and AE effects may determine the direction of easy magnetization, with the former preferring \mathbf{S}_i and \mathbf{S}_j to lie in the plane normal to the \mathbf{D}_{ij} vector and the latter preferring \mathbf{S}_i and \mathbf{S}_j to lie along the largest principal axis (axes) of the $\mathbf{\Gamma}_{ij}$ tensor. The magnitudes of both \mathbf{D}_{ij} and $\mathbf{\Gamma}_{ij}$ can be estimated in terms of t_{00} , U , and the magnitude of Moriya's spin–orbit-mediated transfer parameter $|C_{00}|$ ²⁷ (eq 8).

While the AE term including $\mathbf{\Gamma}_{ij}$ is often neglected,²⁸ it cannot be omitted in the present context because the magnitude of \mathbf{D}_{ij} is decreased as a result of the near-orthogonal overlap of adjacent SOMOs (Figure 3b), which leads to a small value of t_{00} . Indeed, bulk ferromagnetic ordering in **1** is realized only because the slipped π -stacked packing of radicals leads to a small value of t_{00} , which has been estimated from tight-binding band calculations to be no more than 0.01 eV.^{6,8} In contrast, the transfer integrals t_{n0} between the SOMO and other orbitals $|\psi_n\rangle$ (doubly occupied and virtual) on adjacent radicals are not so constrained; we estimate these to be much larger than t_{00} (on the order of 0.1 eV). If we then assume that the molecular spin–orbit coupling constant λ can be represented in terms of the atomic value for selenium (0.1 eV),²⁹ the value of $|C_{00}|$ can be estimated as ~ 0.01 eV;³⁰ setting the on-site Coulomb repulsion U as ~ 0.8 eV (from electrochemical measurements^{6a}), we then arrive at values near 10^{-4} eV for both $|\mathbf{D}_{ij}|$ and $|\mathbf{\Gamma}_{ij}|$. Finally, using $J_{ij} \sim 10^{-3}$ eV (derived from density functional theory calculations^{6,8}) affords an order-of-magnitude estimate of the overall anisotropy constant K in terms of the respective DM and AE contributions K^{DM} and K^{AE} :³¹

$$K = K^{\text{DM}} + K^{\text{AE}} \approx \frac{|\mathbf{D}_{ij}|^2}{J_{ij}} + |\mathbf{\Gamma}_{ij}| \sim 10^{-5} \text{ eV} + 10^{-4} \text{ eV} \quad (9)$$

The order of magnitude of K given by eq 9 is consistent with the experimentally obtained value of 2.4×10^{-5} eV, providing qualitative support for our interpretation of the large anisotropy in terms of a spin–orbit effect. Essentially, the incorporation of the heavy atom selenium leads to a significant increase in spin–orbit coupling and a consequent enhancement of both the DM and AE contributions to the overall anisotropy. If, for example, the value of λ for selenium (0.1 eV) is replaced by that of sulfur (0.02 eV),²⁹ the resulting K^{DM} and K^{AE} values are both smaller by a factor of 25. It is therefore easy to understand qualitatively why the magnetic anisotropy and hence the coercive field of **1** is enhanced relative to that of the mixed S/Se radical **2** ($H_c = 250$ Oe at 2 K) and so much greater than that found in light-element ferromagnets.⁵

In conclusion, we have explored the magnetic properties of the bisdiselenazoyl radical **1** using ferromagnetic resonance absorption methods. The results not only confirm the onset of long-range ferromagnetic order below T_C but are consistent with the exceptionally large coercive field H_c displayed by this nonmetal-based ferromagnet. Preliminary analysis of the symmetry of the DM and AE interactions indicates that both spin–orbit effects should produce an easy c -axis geometry, also consistent with the observations. Taken as a set, materials **1**–**3** offer a unique opportunity to study the competition between DM and AE interactions of similar magnitude. We expect that more detailed

theoretical analysis as well as ongoing experimental studies of compounds **2** and **3** will further illuminate these points.

In a broader context, the present results suggest that large magnetic anisotropies and coercive fields should be considered as natural properties of heavy atom radical ferromagnets, in accord with the early prescription for ferromagnetism provided by Heisenberg.^{5,32} The work also demonstrates that rich spin–orbit physics should not be considered unique to metal-based systems. In view of the technological and theoretical relevance of such physics in spintronics applications,³³ these conclusions serve to encourage continued exploration of heavy p-block radicals and the magnetic materials that can be constructed from them.

AUTHOR INFORMATION

Corresponding Author

oakley@uwaterloo.ca

ACKNOWLEDGMENT

We thank the NSERC of Canada and the U.S. NSF (Grant DMR0804408) for financial support. S.M.W. acknowledges the NSERC for a Canada Graduate Scholarship. The NHMFL is supported by the NSF and by the State of Florida.

REFERENCES

- (1) (a) Rawson, J. M.; Alberola, A.; Whalley, A. J. *Mater. Chem.* **2006**, *16*, 2560. (b) Blundell, S. J. *Contemp. Phys.* **2007**, *48*, 275. (c) Awaga, K.; Tanaka, T.; Shirai, T.; Umezono, Y.; Fujita, W. *C. R. Chim.* **2007**, *10*, 52. (d) Awaga, K.; Tanaka, T.; Shirai, T.; Fujimori, M.; Suzuki, Y.; Yoshikawa, H.; Fujita, W. *Bull. Chem. Soc. Jpn.* **2006**, *79*, 25. (e) Hicks, R. G. In *Stable Radicals: Fundamentals and Applied Aspects of Odd-Electron Compounds*; Hicks, R. G., Ed.; Wiley: Chichester, U.K., 2010; p 317.
- (2) (a) Kinoshita, M.; Turek, P.; Tamura, M.; Nozawa, K.; Shiomi, D.; Nakazawa, Y.; Ishikawa, M.; Takahashi, M.; Awaga, K.; Inabe, T.; Maruyama, Y. *Chem. Lett.* **1991**, 1225. (b) Tamura, M.; Nakazawa, Y.; Shiomi, D.; Nozawa, K.; Hosokoshi, Y.; Ishikawa, M.; Takahashi, M.; Kinoshita, M. *Chem. Phys. Lett.* **1991**, *186*, 401. (c) Chiarelli, R.; Novak, M. N.; Rassat, A.; Tholence, J. L. *Nature* **1993**, *363*, 147. (d) Alberola, A.; Less, R. J.; Pask, C. M.; Rawson, J. M.; Palacio, F.; Ollite, P.; Paulsen, C.; Yamaguchi, A.; Farley, R. D.; Murphy, D. M. *Angew. Chem., Int. Ed.* **2003**, *42*, 4782.
- (3) (a) Fujita, W.; Awaga, K. *Chem. Phys. Lett.* **2002**, *357*, 385. (b) Fujita, W.; Awaga, K. *Chem. Phys. Lett.* **2004**, *388*, 186.
- (4) Allemand, P. M.; Khemani, K. C.; Koch, A.; Wudl, F.; Holczer, K.; Donovan, S.; Gruner, G.; Thompson, J. D. *Science* **1991**, *253*, 301.
- (5) Day, P. *Nature* **1993**, *363*, 113.
- (6) (a) Robertson, C. M.; Leitch, A. A.; Cvrkalj, K.; Reed, R. W.; Myles, D. J. T.; Dube, P. A.; Oakley, R. T. *J. Am. Chem. Soc.* **2008**, *130*, 8414. (b) Robertson, C. M.; Leitch, A. A.; Cvrkalj, K.; Myles, D. J. T.; Reed, R. W.; Dube, P. A.; Oakley, R. T. *J. Am. Chem. Soc.* **2008**, *130*, 14791.
- (7) Beer, L.; Brusso, J. L.; Cordes, A. W.; Haddon, R. C.; Itkis, M. E.; Kirschbaum, K.; MacGregor, D. S.; Oakley, R. T.; Pinkerton, A. A.; Reed, R. W. *J. Am. Chem. Soc.* **2002**, *124*, 9498.
- (8) Leitch, A. A.; Yu, X.; Winter, S. M.; Secco, R. A.; Dube, P. A.; Oakley, R. T. *J. Am. Chem. Soc.* **2009**, *131*, 7112.
- (9) FMR studies were carried out on single crystals of **1** (prepared as described in ref 6a) using several different instruments. The large value of H_A necessitated high-frequency measurements. Orientation- and temperature-dependent studies were performed at multiple frequencies (50–120 GHz) using a superheterodyne-cavity-based spectrometer developed around a Quantum Design PPMS configured with a 7 T split-pair magnet; this spectrometer is described in ref 10. Measurements below 50 GHz were performed in a homodyne transmission instrument

and a commercial X-band (9.7 GHz) spectrometer. Data at 240 GHz were collected using a quasi-optical spectrometer described in ref 11.

- (10) (a) Mola, M.; Hill, S.; Goy, P.; Gross, M. *Rev. Sci. Instrum.* **2000**, *71*, 186. (b) Takahashi, S.; Hill, S. *Rev. Sci. Instrum.* **2005**, *76*, No. 023114.

- (11) Morley, G. W.; Brunel, L. C.; van Tol, J. *Rev. Sci. Instrum.* **2008**, *79*, No. 064703.

- (12) (a) Vonsovskii, S. V. *Ferromagnetic Resonance*; Pergamon Press: London, 1966. (b) Kittel, C. *Introduction to Solid State Physics*, 7th ed.; Wiley: New York, 1996.

- (13) For example, see: Farle, M. *Rep. Prog. Phys.* **1998**, *61*, 775.

- (14) Rawson, J. M.; Alberola, A.; El-Mkami, H.; Smith, G. M. *J. Phys. Chem. Solids* **2004**, *65*, 727.

- (15) The fact that the two are not equal, as simple models predict, is known as Brown's paradox. See: Coey, J. M. D. *Magnetism and Magnetic Materials*; Cambridge University Press: Cambridge, U.K., 2009.

- (16) Arcon, D.; Cevc, P.; Omerzu, A.; Blinc, R. *Phys. Rev. Lett.* **1998**, *80*, 1529. The originally reported value $H_K = 29$ G was modified to reflect the fact that $H_K = H_A/2$.

- (17) Kambe, T.; Kajiyoshi, J.; Oshima, K.; Tamura, M.; Kinoshita, M. *Polyhedron* **2005**, *24*, 2468.

- (18) Ono, F. *J. Phys. Soc. Jpn.* **1981**, *50*, 2564.

- (19) (a) Toukmaji, A. Y.; Board, J. A. *Comput. Phys. Commun.* **1996**, *95*, 73. (b) Wang, Z.; Holm, C. J. *Chem. Phys.* **2001**, *115*, 6351.

- (20) (a) Stanger, J.-L.; André, J.-J.; Turek, P.; Hosokoshi, Y.; Tamura, M.; Kinoshita, M.; Rey, P.; Cirujeda, J.; Veciana, J. *Phys. Rev. B* **1997**, *55*, 8398. (b) Kobayashi, T.; Takiguchi, M.; Amaya, K.; Sugimoto, H.; Kajiwar, A.; Harada, A.; Kamachi, M. *J. Phys. Soc. Jpn.* **1993**, *62*, 3239.

- (21) Dai, D.; Xiang, H.; Whangbo, M.-H. *J. Comput. Chem.* **2008**, *29*, 2187.

- (22) Pivtsov, A. V.; Kulik, L. V.; Makarov, A. Y.; Blockhuys, F. *Phys. Chem. Chem. Phys.* **2011**, *13*, 3873.

- (23) For simplicity, the spin degrees of freedom have been absorbed into the ψ label. This expansion in one-electron states is strictly true only when processes of type 3 (Figure 3), which alter the spin multiplicity of the full electronic state, are neglected. The expansion becomes inappropriate at higher order. For details, see: Yildirim, T.; Harris, A. B.; Aharony, A.; Entin-Wohlman, O. *Phys. Rev. B* **1995**, *52*, 10239.

- (24) Moriya, T. *Phys. Rev.* **1960**, *120*, 91.

- (25) Calzado, C. J.; Cabrero, J.; Malrieu, J. P.; Caballol, R. *J. Chem. Phys.* **2002**, *116*, 2728.

- (26) Leitch, A. A.; Brusso, J. L.; Cvrkalj, K.; Reed, R. W.; Robertson, C. M.; Dube, P. A.; Oakley, R. T. *Chem. Commun.* **2007**, 3368.

- (27) The magnitude of Moriya's spin–orbit-mediated transfer parameter for interactions between SOMOs on adjacent radicals is defined as

$$|C_{00}| = \lambda \left| \sum_{n,m} \frac{\langle \psi_{n,i}^{(0)} | \hat{L}_i \cdot \hat{S}_i | \psi_{0,i}^{(0)} \rangle}{\epsilon_n - \epsilon_0} t_{n0} + \frac{\langle \psi_{0,j}^{(0)} | \hat{L}_j \cdot \hat{S}_j | \psi_{m,j}^{(0)} \rangle}{\epsilon_m - \epsilon_0} t_{0m} \right|$$

where n and m label orbitals on i and j sites, respectively.

- (28) For example, see: Pesin, D.; Balents, L. *Nat. Phys.* **2010**, *6*, 376.

- (29) Blume, M.; Watson, R. E. *Proc. R. Soc. London, Ser. A* **1963**, *271*, 565.

- (30) In this calculation, we set $\epsilon_n - \epsilon_0 \approx 1$ eV and $t_{n0} \approx 0.1$ eV.

- (31) Shekhtman, L.; Entin-Wohlman, O.; Aharony, A. *Phys. Rev. Lett.* **1992**, *69*, 836.

- (32) In Heisenberg's words, "Die Hauptquantenzahl der für den Magnetismus verantwortlichen Elektronen muss $n \geq 3$ sein." See: Heisenberg, W. *Z. Phys.* **1928**, *49*, 619.

- (33) (a) Wolf, S. A.; Awschalom, D. D.; Buhrman, R. A.; Daughton, J. M.; von Molnár, S.; Roukes, M. L.; Chtchelkanova, A. Y.; Trege, B. D. *Science* **2001**, *294*, 1488. (b) Žutić, I.; Fabian, J.; Das Sarma, S. *Rev. Mod. Phys.* **2004**, *76*, 323. (c) Bader, S. D.; Parkin, S. S. P. *Annu. Rev. Condens. Matter Phys.* **2010**, *1*, 71.